Earthquakes and Structures, *Vol. 13, No. 6 (2017) 551-559*
DOI: https://doi.org/10.12989/eas.2017.13.6.551

Effects of friction variability on a rolling-damper-spring isolation system

Biao Wei[1,2a], Peng Wang[1,2b], Xuhui He[*1,2], Zhen Zhang[1,2c] and Liang Chen[3d]

[1]*School of Civil Engineering, Central South University, 22 Shaoshan South Road, Changsha, China*
[2]*National Engineering Laboratory for High Speed Railway Construction, 22 Shaoshan South Road, Changsha, China*
[3]*School of Civil Engineering, Hefei University of Technology, 193 Dunxi Road, Hefei, China*

(Received June 2, 2016, Revised January 13, 2018, Accepted January 16, 2018)

Abstract. A large number of isolation systems are designed without considering the non-uniform friction distribution in space. In order to analyze the effects of non-uniform friction distribution on the structural response of isolation system, this paper presented a simplified rolling-damper-spring isolation system and analyzed the structural responses under earthquakes. The numerical results indicate that the calculation errors related to the peak values of structural acceleration, relative displacement and residual displacement are sequentially growing because of the ignorance of non-uniform friction distribution. However, the influence rule may be weakened by the spring and damper actions, and the unreasonable spring constant may lead to the sympathetic vibration of isolation system. In the case when the friction variability is large and the damper action is little, the non-uniform friction distribution should be taken into consideration during the calculation process of the peak values of structural acceleration and relative displacement. The non-uniform friction distribution should be taken into full consideration regardless of friction variability degree in calculating the residual displacement of isolation system.

Keywords: seismic isolation; friction variability; rolling friction; spring; viscous damper

1. Introduction

Both building and bridge structures are fragile to different degrees of seismic damage in the previous earthquake events. And various kinds of isolation devices, such as laminated rubber bearing and lead rubber bearing, have been widely used for reducing the structural responses during earthquakes. However, those traditional isolation devices are usually limited in the practical application. When the actual seismic ground motion is different from the design value, there will be seismic damages and even resonances in the isolation system. This strange phenomenon has gained wide attention of some researchers (Ismail *et al*. 2015, Siringoringo and Fujino 2015).

In order to attain the optimum seismic performance of isolation system, some scholars have researched on a novel isolation method based on the rolling action in recent years (Wei *et al*. 2017, Wei *et al*. 2018). Harvey and Gavin (2014) carried out a finite element model analysis and experimental validation for double rolling isolation systems (RISs), and evaluated the influence of structure mass, initial conditions, and duration and amplitude of the external disturbance on the seismic performance of isolation system. Furthermore, Harvey *et al*. (2014) proposed a simplified RISs model that could be widely used for all kinds of energy functions. The model was successfully verified by the correct prediction of structural peak responses for extensive disturbance intensities and frequencies. Afterwards, Harvey and Gavin (2015) presented a new kind of reduced-order modeling method to inspect the seismic performances of RISs with light or heavy damping materials. Ismail and Casas (2014a, 2014b) demonstrated that the roll-n-cage (RNC) isolator was useful to protect cable-stayed bridges from the near-fault (NF) earthquakes. Later, Ismail (2015) verified the seismic performance of RNC isolator in near-fault earthquake zones with the consideration of small seismic gaps. Wang *et al*. (2014) found that the isolation devices of sloped multi-roller possessed an exceptional seismic isolation performance for protecting equipments and facilities. Chung *et al*. (2015) claimed that an inappropriate damper may reduce the effectiveness of isolation system, and proposed a theoretical method to achieve an optimal frictional coefficient of isolation system. Ortiz *et al*. (2015) established a finite element model for the dynamic analysis of buildings supported by roller isolation bearings and validated the finite element model by comparing with experimental results.

Before 2014, some similar rolling-based isolation devices also attracted wide concern of several prominent scholars. Jangid and Londhe (1998) generated a numerical equation to access the seismic performance of a multi-story building located on elliptical rolling rods, the analytical results demonstrated that the elliptical rolling rods were conductive to reducing the structural seismic response to

∗Corresponding author, Professor
E-mail: xuhuihe@csu.edu.cn
[a]Associate Professor
E-mail: weibiao@csu.edu.cn
[b]Graduate Research Assistant
E-mail: wangpeng192318@csu.edu.cn
[c]Graduate Research Assistant
E-mail: joyzhen@csu.edu.cn
[d]Associate Professor
E-mail: POPECL@hfut.edu.cn

http://www.techno-press.com/journals/eas&subpage=7 ISSN: 2092-7614 (Print), 2092-7622 (Online)

avoid excessive base displacements. Jangid (2000) analyzed the stochastic response of flexible multi-story shear type buildings isolated by rolling rods with a re-restoring device, indicating that the rolling rods were effectively used to reduce the structural stochastic response under earthquake excitations. Antonyuk and Plakhtienko (2004) investigated the possible states of a system interacting solids with unilateral sliding friction and rolling friction bonds, and identified its application in the seismic isolation of buildings. By using the self-restoring capacity, rolling mechanisms, and certain friction devices for dissipating earthquake energy, Lee *et al*. (2010) firstly applied the roller seismic isolation bearing in the highway bridges. After the parametric studies of bearing's seismic behaviors, Lee *et al*. questioned the correctness of calculation method in AASHTO Specifications and recommended further researches. In 2013, a rolling isolation platform with four pairs of concave steel bowls was built by Harvey and Gavin (2013) to effectively protect the isolated objects from horizontal shaking hazards. Analysis results illustrated that uni-axial models were not suitable to predict system responses. At the same instant, Harvey, Wiebe and Gavin (2013) discovered that chaotic behaviors and impact actions occurred in a similar rolling-pendulum isolation system. Cui (2012) isolated an entire raised floor in a building by using solid polyurethane and rubber balls, and confirmed its practical application. Similarly, Guerreiro *et al.* (2007) proposed a numerical modeling of a rolling-ball isolation system and validated it with a seismic test. The results showed that the rolling-ball isolation system can effectively reduce the structural acceleration levels. With the aim to prolong the service life of isolation system, Tsai (2010) proposed a static dynamics interchangeable-ball pendulum system (SDI-BPS) in 2010. In general, several steel balls are used to support vertical loadings. However, those balls didn't work any more when an earthquake happened. Instead, the damped steel balls start to undertake additional damping force by deforming the surrounded damping materials. Kurita (2011) developed a similar device which could reduce the peak acceleration amplitude of isolated structure by approximate 50-90%. Afterwards, Nanda (2012) regarded the pure friction (P-F) isolation as a good choice to dissipate earthquake energy under strong earthquakes, and the P-F isolation could be utilized easily in the low-cost buildings of brick masonry.

In the above studies, even though the friction isolation device is conductive to reducing the structural seismic damage, the induced displacement of isolation system may be very large and uncontrollable (Kosntantinidis and Makris 2009, Lewis and Murray 1995). And thus a few restoring devices, such as dampers and springs, are used to eliminate excessive relative displacement and residual displacement (Wei *et al*. 2014a, Wei *et al*. 2014b). In order to obtain the excellent isolation performance, the optimum combination of friction device, spring and damper need to be further investigated. Furthermore, aimed at the simplification of computed process for the structural seismic response, the previous applications and researches usually presume all of the friction coefficients to be a certain value, i.e., the friction distribution is absolutely uniform on the entire contact surface (Wei *et al*. 2016, Wei *et al*. 2018). But this assumption is unreasonable to some extent (Wei *et al*. 2013, Wang *et al*. 2010, Yin and Wei 2013). Because of rough contact surface, the corresponding friction coefficient is usually uneven on the contact surface (Begley and Virgin 1998, Flom and Bueche 1959). Theoretically, the uneven friction distribution may result in a few uncertain seismic responses of isolation system (Wei *et al*. 2015, Yim *et al*. 1980). And thus it is necessary to inspect whether the calculation results, including the acceleration, relative displacement and residual displacement of isolation system, based on the original uniform friction assumption are safe, and what the corresponding errors are.

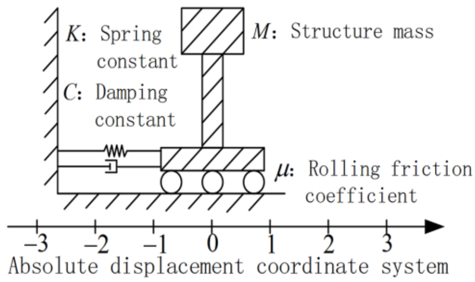

Fig. 1 A rolling-damper-spring isolation system

By taking a rolling-damper-spring isolation system as the study object, this paper compiled a computer program and systematically analyzed the effects of non-uniform friction distribution on the seismic performance of isolation system. The calculation errors due to the ignorance of non-uniform friction distribution in space were summarized.

2. Calculation process

2.1 Structural model

In order to study the isolation method based on the rolling action, Wei *et al*. (2014) wrote a computer program and analyzed the seismic performance of rolling-damper-spring isolation system. This isolation system can be used as an effective device in both bridge and building structures to reduce earthquake energy transferred to superstructure. As shown in Fig. 1, due to the fact that the structural stiffness was much larger than that of isolation device, the isolated structure was presumed to be a rigid body. Besides, the structural mass was set to be 300 ton. The spring constants adopted 200, 400, 600, 800 and 1000 kN·s/m, respectively. The damping constants adopted 100, 200, 300, 400 and 500 kN·s/m, respectively.

With the aim to mathematically describe the motions of structure and ground, the coordinate system of absolute displacement is defined in Fig. 1. The terms d_e, d_s, v_e, v_s, a_e, a_s are defined as the absolute displacement, velocity and acceleration of ground and structure, respectively, and g, μ, K, C, m denote the gravity acceleration, rolling friction coefficient, spring constant, damping constant and mass of structure.

For the rolling-damper-spring isolation system, the equation of motion can be expressed as $ma_e = \pm F_{friction} + K(d_e - d_s) + C(v_e - v_s)$, where $F_{friction}$

Table 1 Eighteen friction distributions on the contact surface

Rolling friction coefficient			Rolling friction coefficient		
Average value E_μ	Cases	Variation coefficient γ_μ	Average value E_μ	Cases	Variation coefficient γ_μ
0.005	Case 1	0	0.020	Case 1	0
	Case 2	0.163		Case 2	0.041
	Case 3	0.471		Case 3	0.118
0.010	Case 1	0	0.025	Case 1	0
	Case 2	0.082		Case 2	0.033
	Case 3	0.236		Case 3	0.094
0.015	Case 1	0	0.030	Case 1	0
	Case 2	0.054		Case 2	0.027
	Case 3	0.157		Case 3	0.079

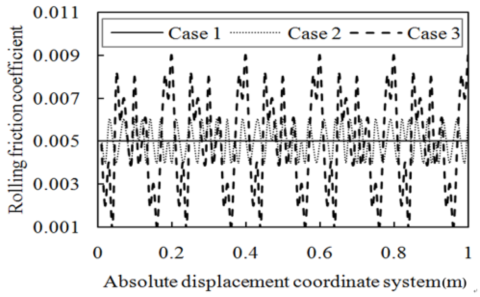

Fig. 2 Three cases of rolling friction coefficient distribution (average value:0.005)

is defined as the friction force on the contact surface of isolation system and $F_{friction} \le \mu mg$. When $v_e > v_s$, it indicates that the ground moves faster than the structure in the coordinate system of Fig. 1, and thus the direction of rolling friction force is consistent with that of the spring force and damping force, resulting in the structural maximum acceleration $[\mu g + K(d_e - d_s) + C(v_e - v_s)/m]$.

As shown in Fig. 1, the structural contact surface respectively adopts 6 average rolling friction coefficients, including 0.005, 0.010, 0.015, 0.020, 0.025 and 0.030. Besides, there are three different friction distribution cases for each average rolling friction coefficient as illustrate in Fig. 2. The variation coefficient γ_μ is defined as $\gamma_\mu = \sigma_\mu / E_\mu$, where σ_μ is the standard deviation of rolling friction coefficient and E_μ is the average value. In total, there are eighteen cases as listed in Table 1. Taking the average rolling friction coefficient of 0.005 in Fig. 2 as example, the non-uniform friction distribution can be randomly adopted with a little or wide range of fluctuation around its average value. So the friction distribution can be divided into three cases:

Case 1 (uniform friction distribution): the traditional assumptions assume that the rolling friction coefficient remains a fixed value regardless of different positions on contact surface, i.e., the friction distribution is uniform on the contact surface.

Case 2 (slightly non-uniform friction distribution): the friction distribution slightly changes near the average rolling friction coefficient with a little variable range of –0.001~0.001 when the position on a perfectly constructed contact surface changes.

Case 3 (significantly non-uniform friction distribution): with regard to a poorly constructed contact surface, the friction distribution significantly changes with a wide range of fluctuation near the average rolling friction coefficient and the variable range is -0.004~0.004.

Table 2 Combination rule of the structural parameters

Rolling friction coefficient		Spring constants	Damping constants	Accelerograms	PGA
One average value	Case 1	Combined with the same spring constant	Combined with the same damping constant	Subjected to the same accelerogram	With the same PGA
	Case 2				
	Case 3				

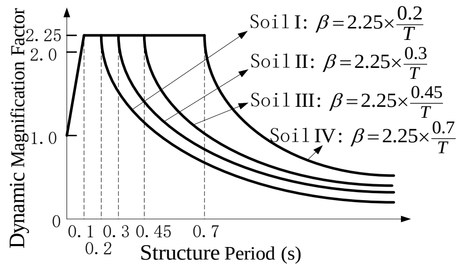

(a) Elastic response spectrum for different soil profiles in Chinese criteria (JTJ 004-89)

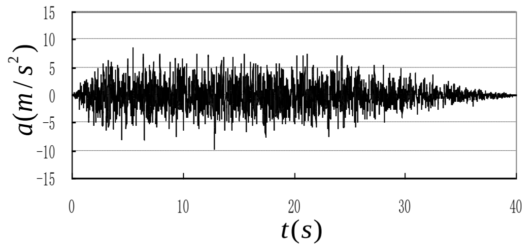

(b) A representative accelerogram corresponding to the soil profile I

Fig. 3 Ground motion

2.2 Ground motion

According to the response spectrums for different soil profiles in Chinese criteria as illustrated in Fig. 3(a) (JTJ 004-89) (1989), four accelerograms are produced by using Simqke procedure (Fahjan and Ozdemir, 2008). One representative ground motion out of four is shown in Fig. 3(b). Other motions are calculated but not presented herein due to the similarity to Fig. 3(b). In the further calculation, each accelerogram's peak ground accelerations (PGA) are adjusted to be 0.2, 0.4, 0.6 and 0.8g, respectively. In the end, all accelerograms are input into the isolation system as the ground motion inputs.

2.3 Calculation cases

In this paper, there are 18 friction distributions, 5 spring constants, 5 damping constants, 4 soil profile accelerograms and 4 PGAs. Totally, there are 7200 calculation cases, and the combination rule is shown in Table 2.

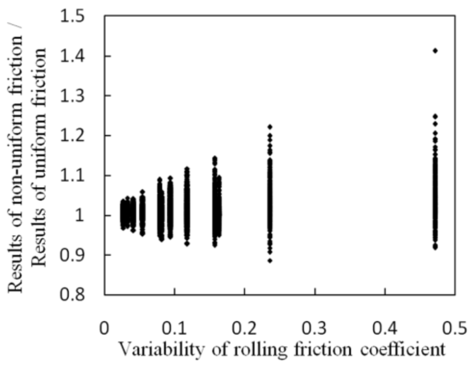

(a) Influence of friction variability

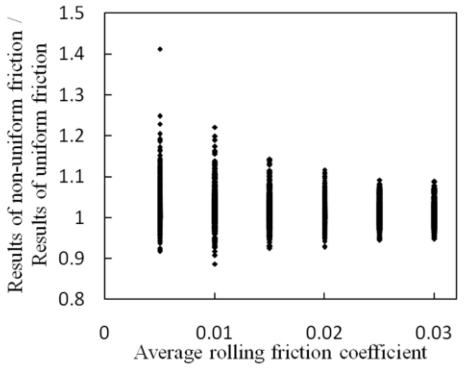

(b) Influence of average rolling friction coefficient

Fig. 4 Effects of non-uniform friction distribution on the peak acceleration of isolation system

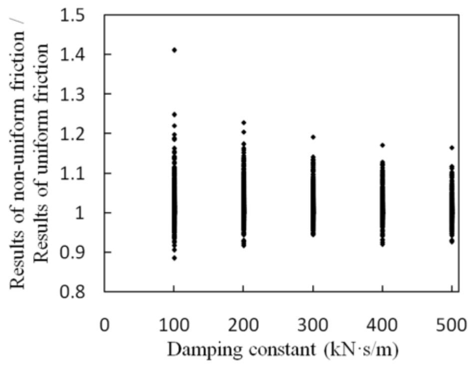

Fig. 5 Effects of damping constant on the peak acceleration of isolation system

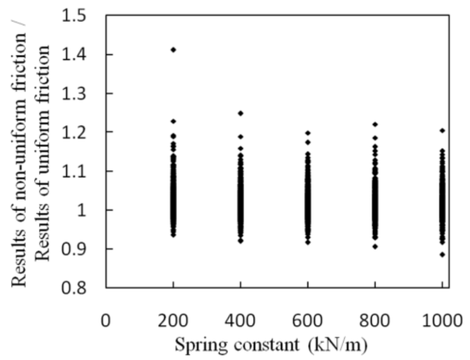

Fig. 6 Effects of spring constant on the peak acceleration of isolation system

In terms of each average rolling friction coefficient corresponding to cases 2 and 3 in Table 2, the actual distribution of rolling friction coefficient should be taken into strict consideration, and the proportions of the calculation results of cases 2 and 3 to that of case 1 will be analyzed to investigate the influence of non-uniform friction distribution on the system's seismic performance. The calculation results include the peak values of acceleration, relative displacement and residual displacement for the isolation system. And there are four influence factors, i.e. the non-uniform friction distribution, spring constant, damping constant and different ground motions. All of these influence factors are calculated and analyzed in the following sections 3, 4 and 5.

3. Peak acceleration of isolation system

3.1 Effects of non-uniform friction distribution

Fig. 4(a) illustrates the effects of non-uniform friction distribution on the peak acceleration responses of isolation system. As the friction variability increases, the variable range of the peak acceleration proportions of the non-uniform friction results to the uniform counterpart becomes larger and worse. The peak acceleration proportion even surges to 1.43 when the friction variability is 0.471 in space. It means that the peak acceleration of isolation system is underestimated and its calculated value is 43% less than the accurate value if the non-uniform friction distribution is ignored. Therefore, the non-uniform friction distribution should be taken into account when calculating the peak acceleration responses.

According to the present construction technology, the amplitude of friction variability on the contact surface can be limited in a small range no matter how large the average rolling friction coefficient is. Hence, as the average rolling friction coefficient becomes larger, both the friction variability on the contact surface and the peak acceleration proportions of the non-uniform friction results to the uniform counterpart become smaller, which are illustrated in Fig. 4(b).

3.2 Effects of viscous damping constant

In Fig. 5, as the viscous damping constant becomes larger, the variable range of the peak acceleration proportions of the non-uniform friction results to the uniform counterpart becomes smaller. Obviously, all peak acceleration proportions are smaller than 1.2 when the damping constant is beyond 300 kN·s/m.

This influence rule can be explained as follows:

(1) If μ becomes larger, the rapid increment of v_s will significantly reduce $(v_e - v_s)$. Hence, μg shows a reverse trend to $C(v_e - v_s)/m$, which reduces the increasing of $[\mu g + K(d_e - d_s) + C(v_e - v_s)/m]$.

(2) If μ becomes smaller, μg also shows an opposite trend to $C(v_e - v_s)/m$, which reduces the decreasing of $[\mu g + K(d_e - d_s) + C(v_e - v_s)/m]$.

Therefore, the influence rule of non-uniform friction distribution on the peak acceleration responses is weakened as the viscous damping constant increases.

3.3 Effects of spring constant

In Fig. 6, as the spring constant becomes larger, the variable range of the peak acceleration proportions of the non-uniform friction results to the uniform counterpart becomes smaller, however, with some particular points.

This influence rule of non-uniform friction distribution on the peak acceleration responses is weakened as the spring constant increases:

(1) If μ becomes larger, the rapid increment of d_s will significantly reduce $(d_e - d_s)$. Hence, μg shows a reverse trend to $K(d_e - d_s)$, which reduces the increasing of $[\mu g + K(d_e - d_s) + C(v_e - v_s)/m]$.

(2) If μ becomes smaller, μg shows an opposite trend to $K(d_e - d_s)$, which reduces the decreasing of $[\mu g + K(d_e - d_s) + C(v_e - v_s)/m]$.

3.4 Effects of different ground motions

In Figs. 7(a)-(b), as the earthquake soil profile becomes softer and PGA is larger, the peak acceleration proportions of the non-uniform friction results to the uniform counterpart are generally reduced.

Based on the structural dynamic principle, the uniform motion in the identical direction is conductive to strengthening the spring and damper actions, and thus weakening the effects of non-uniform friction distribution. This tendency can be obtained in the following two cases:

(1) As the earthquake soil profile is softer, the duration of ground motion will be prolonged in the identical direction.

(2) As the PGA increases, the absolute displacement of ground motion will be much larger and the isolated structure will be further away from the original position during the same time.

In the above two conditions, the effects of non-uniform friction distribution on the peak acceleration responses of isolation system is reduced.

3.5 Discussion

As the rolling friction coefficient μ changes when the isolation system moves close to or away from the original position, the structural acceleration subsequently changes near $[\mu_{av} g + K(d_e - d_s) + C(v_e - v_s)/m]$ where μ_{av} is the average value of rolling friction coefficient. Hence, the peak acceleration response of isolation system $[\mu_{max} g + K(d_e - d_s) + C(v_e - v_s)/m]$ must change near the average acceleration $[\mu_{av} g + K(d_e - d_s) + C(v_e - v_s)/m]$. Moreover, it is interesting to note that a larger friction variability must lead to a wider variable range of the proportion of $[\mu_{max} g + K(d_e - d_s) + C(v_e - v_s)/m]$ to $[\mu_{av} g + K(d_e - d_s) + C(v_e - v_s)/m]$.

This influence rule is diminished in the following phenomena:

(1) If μ is larger, v_s will significantly increase, so that $(v_e - v_s)$ and $(d_e - d_s)$ are markedly reduced. Hence, μg shows a reverse trend to $C(v_e - v_s)/m$ and $K(d_e - d_s)$, which decreases the increment of $[\mu g + K(d_e - d_s) + C(v_e - v_s)/m]$.

(2) If μ is smaller, μg shows an opposite trend to $C(v_e - v_s)/m$ and $K(d_e - d_s)$, which decreases the reduction of $[\mu g + K(d_e - d_s) + C(v_e - v_s)/m]$.

Therefore, the influence rule of non-uniform friction distribution on the acceleration responses of isolation system will be weakened as the spring constant and damping constant gradually increase.

However, if the spring is strong enough, the isolation structure can be simplified as a conventional isolation system. As the rolling friction coefficient μvaries around the average rolling friction coefficient μ_{av}, the vibration period of isolation system may approach to some earthquake periodic components. Under the circumstances, there will be some fluctuated peak acceleration proportions in Fig. 6. The phenomenon is extremely obvious in the case of a large spring constant, a little damping constant, a little average rolling friction and a large friction variability.

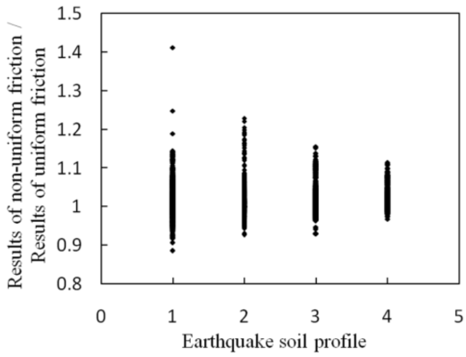

(a) Influence of earthquake soil profile

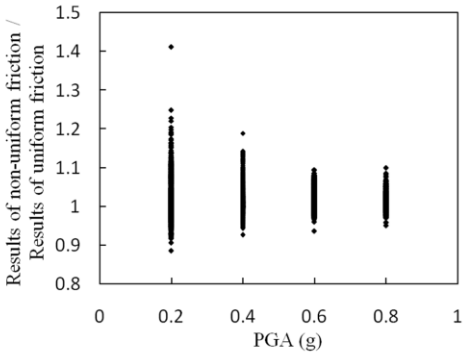

(b) Influence of PGA

Fig. 7 Effects of different ground motions on the peak acceleration of isolation system

4. Peak relative displacement of isolation system

4.1 Effects of non-uniform friction distribution

In Fig. 8(a), as the friction variability increases, the peak relative displacement proportions of the non-uniform friction results to the uniform counterpart becomes larger.

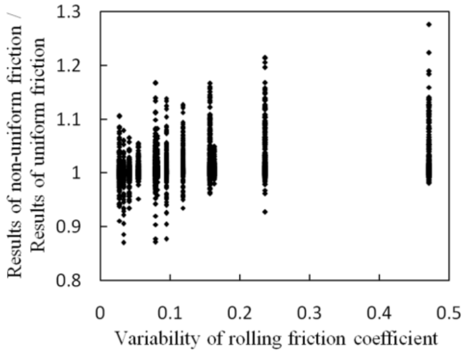

(a) Influence of friction variability

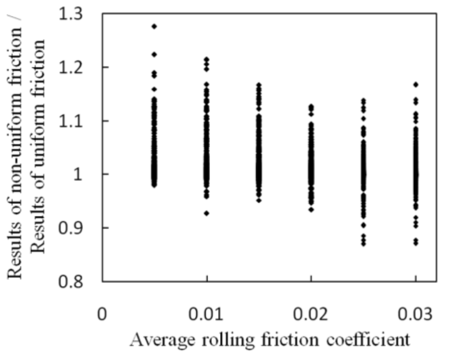

(b) Influence of average rolling friction coefficient

Fig. 8 Effects of non-uniform friction distribution on the peak relative displacement of isolation system

When the friction variability is 0.471, the peak relative displacement proportion reaches 1.28, i.e., the peak relative displacement of isolation system is underestimated and its calculated value is 28% less than the exact one because of the ignorance of non-uniform friction distribution. Hence, the non-uniform friction distribution should be taken into consideration for the sake of accurate peak relative displacement response results.

When the average rolling friction coefficient gradually becomes larger on the generally constructed contact surface, the friction variability will be reduced. And thus the variable range of peak relative displacement proportions in Fig. 8(b) will be much smaller.

4.2 Effects of damping constant

In Fig. 9, as the viscous damping constant C becomes larger, the variable range of the peak relative displacement proportions of the non-uniform friction distribution results to the uniform counterpart is much smaller. However, this rule is not very obvious.

4.3 Effects of spring constant

In Fig. 10, as the spring constant becomes larger, the variable range of the peak relative displacement proportions of the non-uniform friction distribution results to the uniform counterpart becomes smaller. However, there are still some special points exhibited in Fig. 10 as well as in Fig. 6 because of the structural sympathetic vibration.

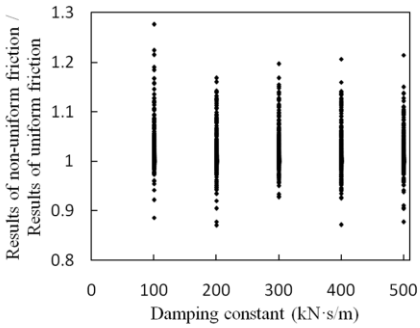

Fig. 9 Effects of damping constant on the peak relative displacement of isolation system

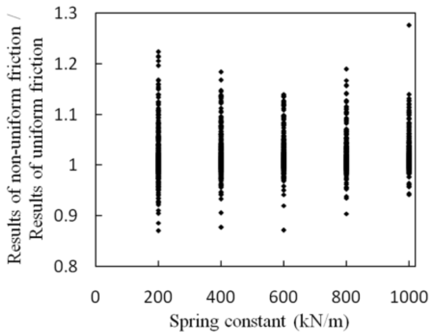

Fig. 10 Effects of spring constant on the peak relative displacement of isolation system

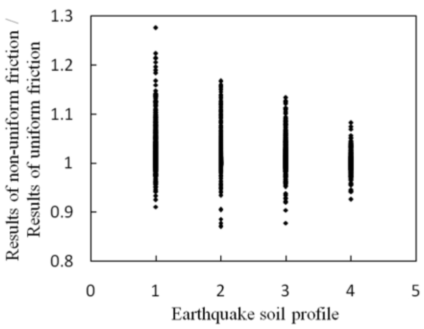

(a) Influence of earthquake soil profile

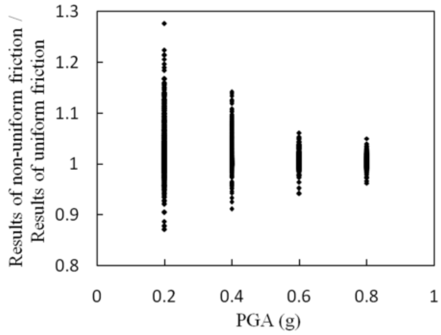

(b) Influence of PGA

Fig. 11 Effects of different ground motions on the relative displacement of isolation system

4.4 Effects of different ground motions

The increasing of earthquake soil profile number and PGA will result in more uniform motion in the identical

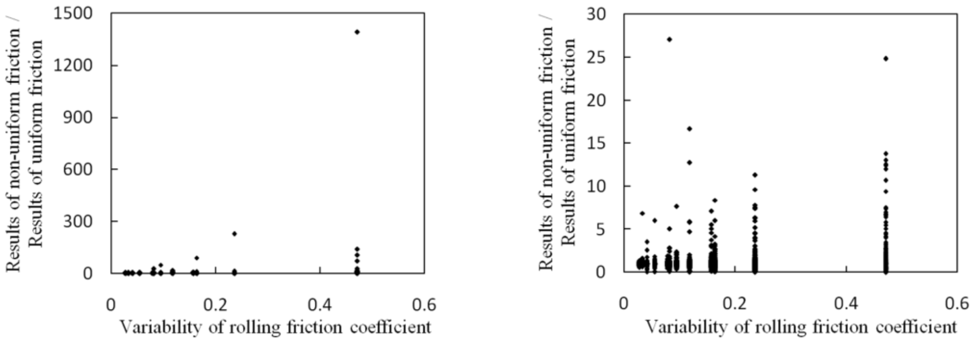

(a1) All cases (a2) Main cases

(a) Influence of friction variability

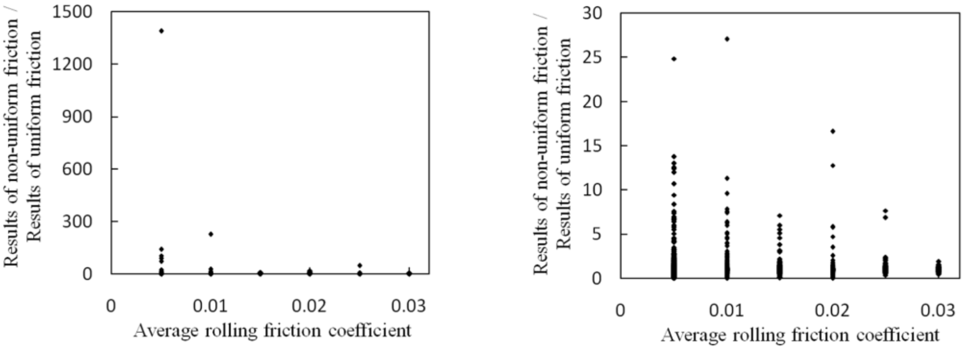

(b1) All cases (b2) Main cases

(b) Influence of average rolling friction coefficient

Fig.12 Effects of non-uniform friction distribution on the residual displacement of isolation system

direction, which strengthens the spring and damper actions and weakens the influence of non-uniform friction distribution. As the earthquake soil profile is softer and PGA is larger, the peak displacement proportions in Figs. 11(a)-(b) will be obviously reduced.

4.5 Discussion

In Fig. 1, when the absolute velocity of ground motion v_e becomes larger than the absolute velocity of isolated structure v_s, the system's acceleration $[\mu g + K(d_e - d_s) + C(v_e - v_s)/m]$ makes the structure trend to move forward, and there are two possible cases:

(1) If the isolated structure is on the left of initial position, the increasing of rolling friction coefficient μ will lead to the increasing of peak acceleration $[\mu g + K(d_e - d_s) + C(v_e - v_s)/m]$, and thus reducing the peak relative displacement of isolation system. Otherwise, the peak relative displacement of isolation system will become larger.

(2) Supposing that the isolation system is on the right of initial position, as the rolling friction coefficient μ increases or decreases, the peak relative displacement of isolation system will change in a direction opposite to the variable trends in case (1).

Similar results will be obtained when $v_e = v_s$ and $v_e < v_s$. In general, the non-uniform friction distribution is conductive to increasing or decreasing the peak relative displacement of isolation system under different conditions. And the increasing of friction variability will result in a more significant influence degree and a wider variable range of relative displacement proportion as demonstrated in Fig. 7(a).

According to the discussion in section 3.5, the influence of non-uniform friction distribution on the peak acceleration responses may be weakened by the damper and spring, and thus the influence on the peak relative displacement of isolation system is subsequently weakened. Therefore, as the damping constant C and spring constant K gradually increase, the variable range of the peak relative displacement proportions of the non-uniform friction distribution results to the uniform counterpart will be reduced. However, the stronger spring will make the system's vibration period approach to the earthquake's certain periodic components and result in the sympathetic vibrations of isolation system. The phenomenon is apparent in the condition of a little damper constant, a little average rolling friction coefficient and a large friction variability.

Furthermore, the influence rules of spring constant K and damping constant C are often broken by the specific accelerogram shape, contributing to some particular points in Figs. 8-10 (Wei *et al*. 2015, Wei *et al*. 2016, Wei *et al*. 2017, Jiang *et al*. 2017). The relation between the detailed accelerogram shape and the structural response is still unsolved and studied by researchers. However, as the earthquake soil profile is softer and PGA is larger, the uniform motion will be prolonged in the same direction. And thus the spring action will be strengthened and the influence of non-uniform friction distribution will be weakened.

5. Residual displacement of isolation system

5.1 Effects of non-uniform friction distribution

Fig. 12(a) indicates the effects of non-uniform friction distribution on the residual displacement proportions of non-uniform friction distribution results to the uniform counterpart. As the friction variability is larger, the range of main proportions in Fig. 12(a2) becomes wider while the variable range of most proportions in Fig. 12(a1) is much wider because of some particular points. A particular point even reaches 1400, which indicates that the calculated value of structural residual displacement corresponding to the assumption of uniform friction distribution is 140000% less than the exact value of structural residual displacement corresponding to the real non-uniform friction distribution. Hence, the non-uniform friction distribution should be fully considered during the calculation process of the residual displacement of isolation system. Any simplification of non-uniform friction distribution may lead to significant errors.

Because the residual displacement of isolation system is defined as a particular relative displacement when the isolation system stops moving, the influence of non-uniform friction distribution on the peak relative displacement responses will naturally affect the residual displacement of isolation system. Besides, the residual displacement responses are also affected by the moving direction of isolation system at the moment just when the ground motion stops moving:

(1) If the isolation system leaves the initial position, the residual displacement of isolation system shows an opposite variation trend to the non-uniform friction distribution.

(2) Otherwise, the residual displacement responses will keep a consistent variation trend with the non-uniform friction distribution.

According to the above influence factors, the effects of non-uniform friction distribution on the residual displacement of isolation system are much larger than that on the peak relative displacement responses.

As illustrated in Fig. 12(b), as the average rolling friction coefficient becomes larger, both the variable range of residual displacement proportions and the friction variability are reduced. However, the maximum residual displacement proportion still reaches 2.0 when the average rolling friction coefficient is 0.03.

5.2 Effects of other factors

The larger spring constant will lead to the sympathetic vibration of isolation system, however, the increasing or decreasing of μ will make the vibration period of isolation system tend to be close to or away from some periodic components of earthquake and thus change the conditions of potential sympathetic vibrations. Therefore, the increasing of spring constant will result in a definite trend or even disorder for the residual displacement proportions of non-uniform friction distribution results to the uniform counterpart. Those irregular figures are plotted but not listed herein because of the limited space.

Due to the fact that the damper, earthquake soil profile and PGA are not able to restore the isolated structure to the initial position, they will not have significant effects on the variable range of the residual displacement proportions of non-uniform friction distribution results to the uniform counterpart. Therefore, the corresponding figures are not presented herein.

6. Conclusions

In order to investigate the isolation performance of rolling-damper-spring system under earthquakes, this paper analyzed the effects of non-uniform friction distribution on the structural seismic responses by using a complied computer program. The conclusions are summarized as follows:

- If the non-uniform friction distribution is ignored, it may lead to the sequentially growing errors for the peak acceleration, peak relative displacement and residual displacement of isolation system. This influence rule is diminished by the damper and spring actions. Nevertheless, an unsuitable spring constant may result in structural sympathetic vibrations.
- On the conditions of small friction variability and the conditions of large friction variability and large damping constant, the non-uniform friction distribution can be ignored during the calculation process of the peak relative displacement and peak acceleration of isolation system. However, the influence of non-uniform friction distribution should be fully considered during the calculation process of residual displacement responses.
- As for the calculation cases of large friction variability and little damping constant, the non-uniform friction distribution must be adequately considered to assure the accurate seismic responses of isolation system.

Acknowledgements

The research described in this paper was financially supported by the National Key R&D Program of China under grant No. 2017YFB1201204, the Natural Science Foundations of Hunan Province under grant No. 2015JJ3159, the Innovation-driven Plan in Central South University under grant No. 2015CX006, the Graduate Innovative Project in Central South University under grant No. 2017zzts524 and the Aseismic Software Development of Urban Transit Bridges Based on Capacity Protection Design Method under grant No. 2014D07. The above financial support is greatly appreciated.

References

Antonyuk, E.Y. and Plakhtienko, N.P. (2004), “Dynamic modes of one seismic-damping mechanism with frictiona bonds”, *Int. Appl. Mech.*, **40**(6), 702-708.

Begley, C.J. and Virgin, L.N. (1998), “Impact response and the influence of friction”, *J. Sound Vib.*, **211**(5), 801-818.

Chung, L.L., Kao, P.S., Yang, C.Y., Wu, L.Y. and Chen, H.M. (2015), “Optimal frictional coefficient of structural isolation system", *J. Vib. Control*, **21**(3), 525-538.

Cui, S. (2012), *Integrated Design Methodology for Isolated Floor Systems in Single-Degree-of-Freedom Structural Fuse Systems*, State University of New York, Buffalo.

Fahjan, Y. and Ozdemir, Z. (2008), "Scaling of earthquake accelerograms for non-linear dynamic analysis to match the earthquake design spectra", *The 14th World Conference on Earthquake Engineering*, Chinese Society for Earthquake Engineering, Beijing, China.

Flom, D.G. and Bueche, A.M. (1959), "Theory of rolling friction for spheres", *J. Appl. Phys.*, **30**(11), 1725-1730.

Guerreiro, L., Azevedo, J. and Muhr, A.H. (2007), "Seismic tests and numerical modeling of a rolling-ball isolation system", *J. Earthq. Eng.*, **11**(1), 49-66.

Harvey, P.S. and Gavin, H.P. (2013), "The nonholonomic and chaotic nature of a rolling isolation system", *J. Sound Vib.*, **332**(14), 3535-3551.

Harvey, P.S. and Gavin, H.P. (2014), "Double rolling isolation systems: a mathematical model and experimental validation", *Int. J. Nonlin. Mech.*, **61**(1), 80-92.

Harvey, P.S. and Gavin, H.P. (2015), "Assessment of a rolling isolation system using reduced order structural models", *Eng. Struct.*, **99**, 708-725.

Harvey, P.S., Wiebe, R. and Gavin, H.P. (2013), "On the chaotic response of a nonlinear rolling isolation system", *Physica D: Nonlin. Phenomena*, **256-257**, 36-42.

Harvey, P.S., Zehil, G.P. and Gavin, H.P. (2014), "Experimental validation of a simplified model for rolling isolation systems", *Earthq. Eng. Struct. Dyn.*, **43**(7), 1067-1088.

Ismail, M. (2015), "An isolation system for limited seismic gaps in near-fault zones", *Earthq. Eng. Struct. Dyn.*, **44**(7), 1115-1137.

Ismail, M. and Casas, J.R. (2014), "Novel isolation device for protection of cable-stayed bridges against near-fault earthquakes", *J. Bridge Eng.*, **19**(8), 50-65.

Ismail, M., Rodellar, J. and Pozo, F. (2014), "An isolation device for near-fault ground motions", *Struct. Control Hlth. Monit.*, **21**(3), 249-268.

Ismail, M., Rodellar, J. and Pozo, F. (2015), "Passive and hybrid mitigation of potential near-fault inner pounding of a self-braking seismic isolator", *Soil Dyn. Earthq. Eng.*, **69**(2), 233-250.

Jangid, R.S. (2000), "Stochastic seismic response of structures isolated by rolling rods", *Eng. Struct.*, **22**(8), 937-946.

Jangid, R.S. and Londhe, Y.B. (1998), "Effectiveness of elliptical rolling rods for base isolation", *J. Struct. Eng.*, **124**(4), 469-472.

Jiang, C.W., Wei, B., Wang, D.B., Jiang, L.Z. and He, X.H. (2017), "Seismic vulnerability evaluation of a three-span continuous beam railway bridge", *Math. Prob. Eng.*, **4**, 1-13.

JTJ004-89, Standard of the Ministry of Communications of P.R. China (1989), *Specifications of Earthquake Resistant Design for Highway Engineering*, China Communications Press, Beijing (in Chinese).

Kosntantinidis, D. and Makris, N. (2009), "Experimental and analytical studies on the response of freestanding laboratory equipment to earthquake shaking", *Earthq. Eng. Struct. Dyn.*, **38**(6), 827-848.

Kurita, K., Aoki, S., Nakanishi, Y., Tominaga, K. and Kanazawa, M. (2011), "Fundamental characteristics of reduction system for seismic response using friction force", *J. Civil Eng. Arch.*, **5**(11), 1042-1047.

Lee, G.C., Ou, Y.C., Niu, T.C., Song, J.W. and Liang, Z. (2010), "Characterization of a roller seismic isolation bearing with supplemental energy dissipation for highway bridges", *J. Struct. Eng.*, **136**(5), 502-510.

Lewis, A.D. and Murray, R.M. (1995), "Variational principles for constrained systems: Theory and experiment", *Int. J. Nonlin. Mech.*, **30**(6), 793-815.

Nanda, R.P., Agarwal, P. and Shrikhande, M. (2012), "Base isolation system suitable for masonry buildings", *Asian J. Civil Eng. (Build. Hous.)*, **13**(2), 195-202.

Ortiz, N.A., Magluta, C. and Roitman, N. (2015), "Numerical and experimental studies of a building with roller seismic isolation bearings", *Struct. Eng. Mech.*, **54**(3), 475-489.

Ou, Y.C., Song, J.W. and Lee, G.C. (2010), "A parametric study of seismic behavior of roller seismic isolation bearings for highway bridges", *Earthq. Eng. Struct. Dyn.*, **39**(5), 541-559.

Siringoringo, D.M. and Fujino, Y. (2015), "Seismic response analyses of an asymmetric base-isolated building during the 2011 Great East Japan (Tohoku) Earthquake", *Struct. Control Hlth. Monit.*, **22**(1), 71-90.

Tsai, C.S., Lin, Y.C., Chen, W.S. and Su, H.C. (2010), "Tri-directional shaking table tests of vibration sensitive equipment with static dynamics interchangeable-ball pendulum system", *Earthq. Eng. Eng. Vib.*, **9**(1), 103-112.

Wang, S.J., Hwang, J.S., Chang, K.C., Shiau, C.Y., Lin, W.C., Tsai, M.S., Hong, J.X. and Yang, Y.H. (2014), "Sloped multi-roller isolation devices for seismic protection of equipment and facilities", *Earthq. Eng. Struct. Dyn.*, **43**(10), 1443-1461.

Wang, Y.J., Wei, Q.C., Shi, J. and Long, X.Y. (2010), "Resonance characteristics of two-span continuous beam under moving high speed trains", *Latin Am. J. Solid. Struct.*, **7**(2), 185-199.

Wei, B., Cui, R.B. and Dai, G.L. (2013), "Seismic performance of a rolling-damper isolation system", *J. Vibroeng.*, **15**(3), 1504-1512.

Wei, B., Dai, G.L., Wen, Y. and Xia, Y. (2014), "Seismic performance of an isolation system of rolling friction with spring", *J. Central South Univ.*, **21**(4), 1518-1525.

Wei, B., Wang, P., He, X.H. and Jiang, L.Z. (2016), "Seismic isolation characteristics of a friction system", *J. Test. Eval.*, DOI: 10.1520/JTE20160598.

Wei, B., Wang, P., He, X.H. and Jiang, L.Z. (2018), "The impact of the convex friction distribution on the seismic response of a spring-friction isolation system", *KSCE J. Civil Eng.*, **22**(4), DOI: 10.1007/s12205-017-0938-6.

Wei, B., Wang, P., Liu, W.A., Yang, M.G. and Jiang, L.Z. (2016), "The impact of the concave distribution of rolling friction coefficient on the seismic isolation performance of a spring-rolling system", *Int. J. Nonlin. Mech.*, **83**, 65-77.

Wei, B., Wang, P., Yang, M.G. and Jiang, L.Z. (2017), "Seismic response of rolling isolation systems with concave friction distribution", *J. Earthq. Eng.*, **21**(3), 325-342.

Wei, B., Xia, Y. and Liu, W.A. (2014), "Lateral vibration analysis of continuous bridges utilizing equal displacement rule", *Latin Am. J. Solid. Struct.*, **11**(1), 75-91.

Wei, B., Yang, T.H. and Jiang, L.Z. (2015), "Influence of friction variability on isolation performance of a rolling-damper isolation system", *J. Vibroeng.*, **17**(2), 792-801.

Wei, B., Yang, T.H., Jiang, L.Z. and He X.H. (2017), "Effects of friction-based fixed bearings on the seismic vulnerability of a high-speed railway continuous bridge", *Adv. Struct. Eng.*, DOI: 10.1177/1369433217726894.

Wei, B., Zuo C.J., He, X.H. and Jiang, L.Z. (2018), "Numerical investigation on scaling a pure friction isolation system for civil structures in shaking table model tests", *Int. J. Nonlin. Mech.*, **98**, 1-12.

Yim, C.S., Chopra, A.K. and Penzien, J. (1980), "Rocking response of rigid blocks to earthquakes", *Earthq. Eng. Struct. Dyn.*, **8**(6), 565-587.

Yin, C.F. and Wei, B. (2013), "Numerical simulation of a bridge-subgrade transition zone due to moving vehicle in Shuohuang heavy haul railway", *J. Vibroeng.*, **15**(2), 1062-1068.

CC